

Electronic Supplementary Information

ZIF-67 Nanocubes with Complex Structures Co-mediated by Dopamine and Polyoxometalate

Hao Bin Wu,^a Bu Yuan Guan,^b Peilei He,^{b,*} and Xin-Yao Yu^{a,*}

^aSchool of Materials Science & Engineering, Zhejiang University, Hangzhou 310027, (P. R. China)

Email: yuxinyao@zju.edu.cn

^bSchool of Chemical and Biomedical Engineering, Nanyang Technological University, 62 Nanyang Drive, Singapore 637459 (Singapore)

Email: peileihe@gmail.com

Experimental section

Synthesis of ZIF-67 nanocubes. The ZIF-67 nanocubes were synthesized according to the reference (*Chem* **2016**, *1*, 102). In a typical synthesis, 58 mg of $\text{Co}(\text{NO}_3)_2 \cdot 6\text{H}_2\text{O}$ was dissolved in 2 mL of deionized water containing 1 mg of cetrimonium bromide (CTAB). Then this solution was rapidly injected into 14 mL of aqueous solution containing 908 mg of 2-methylimidazole and stirred at room temperature for 20 min. The product was collected by centrifugation and washed by ethanol for six times.

Synthesis of ZIF-67 nanoscaffolds. First, 15 mg of ZIF-67 nanocubes and 5 mg of dopamine were dispersed into a Tris-buffer solution (10 mL, 10 mM) with magnetic stirring. Then a $\text{H}_3\text{PMo}_{12}\text{O}_{40}$ solution (5 mL, 20 mg) was added. Finally, the mixture was stirred for 10 min. The resultant product was collected via centrifugation and washed three times with ethanol.

Synthesis of ZIF-67 magic nanocubes. First, 45 mg of ZIF-67 nanocubes and 2.5 mg of dopamine were dispersed into a Tris-buffer solution (5 mL, 10 mM). Then a solution of $\text{H}_3\text{PMo}_{12}\text{O}_{40}$ (2.5 mL, 10 mg) was added. Finally, the mixture was stirred for 30 min. The resultant product was collected via centrifugation and washed three times with ethanol.

Synthesis of PDA@ZIF-67 nanocubes. 15 mg of ZIF-67 nanocubes and 5 mg of dopamine were dispersed into a Tris-buffer solution (10 mL, 10 mM) with magnetic stirring for 15 min. The resultant

product was collected via centrifugation and washed three times with ethanol.

Synthesis of POM-PDA hollow nanospheres. The sample was prepared by adding 1 mL of $\text{H}_3\text{PMo}_{12}\text{O}_{40}$ aqueous solution (10 mg/mL) to 0.8 mL of dopamine aqueous solution (2.5 mg/mL). The transparent solution became green immediately and showed turbid within 2 min. After aging for 12 h, the yellow precipitation was collected by removing upper-phase, washing with ethanol for three times.

Synthesis of CoMoSe@C nanoscaffolds. The as prepared POM&PDA@ZIF-67 nanoscaffolds were further annealed with Se powder at 600 °C for 2 h with a ramping rate of 10 °C min⁻¹ under a flow of nitrogen gas.

Synthesis of CoSe₂@C nanoboxes. The as prepared PDA@ZIF-67 nanoboxes were further annealed with Se powder at 600 °C for 2 h with a ramping rate of 10 °C min⁻¹ under a flow of nitrogen gas.

Synthesis of MoSe₂@C hollow nanospheres. The as prepared POM-PDA hollow nanospheres were further annealed with Se powder at 600 °C for 2 h with a ramping rate of 10 °C min⁻¹ under a flow of nitrogen gas.

Materials characterizations. The morphologies of the products were characterized by field-emission scanning electron microscope (FESEM; JEOL-6700F) and transmission electron microscope (TEM; JEOL, JEM-1400). The composition of the samples was characterized by Energy-dispersive X-ray spectroscopy (EDX) attached to the FESEM. X-ray diffraction (XRD) patterns of the products were collected on a Bruker D2 Phaser X-Ray Diffractometer with Cu K α radiation ($\lambda = 1.5406 \text{ \AA}$). HRTEM images, HAADF-STEM images and elemental mapping were collected using a TEM (JEOL, JEM-2100F) equipped with EDX spectroscopy. Raman spectra were collected on a Renishaw Invia Reflex Raman microscope equipped with a 514 nm excitation laser.

Electrochemical measurements. The electrode film was prepared by pasting the slurry containing 80 wt.% of active materials (CoMoSe@C nanoscaffold, CoSe₂@C nanoboxes, or MoSe₂@C hollow nanospheres), 10 wt.% of conductive carbon (super-P) and 10 wt.% sodium carboxymethyl cellulose (NaCMC) binder onto a copper foil. The electrode film was dried in a vacuum oven at 80 °C overnight. The average areal mass loading of the active materials on electrodes was about 1.0 mg cm⁻². The 2032-type coin cells were assembled using Celgard 2300 membrane as separator. The electrolyte was a 1.0 M LiPF₆ in a mixture of ethylene carbonate and diethyl carbonate (1: 1 by vol.) solution. Lithium thin disks were used as counter electrodes. All the cells were assembled in an argon-filled glovebox with

content of water/oxygen below 1.0 ppm. The galvanostatic charge/discharge tests were conducted over a voltage range of 0.01-3.0 V versus Li/Li⁺ on a LAND battery tester. Cyclic voltammetry (CV) tests were conducted on a CHI 660D electrochemical workstation. Electrochemical impedance spectroscopy (EIS) measurements were performed over the frequency range of 100,000 Hz to 0.1 Hz.

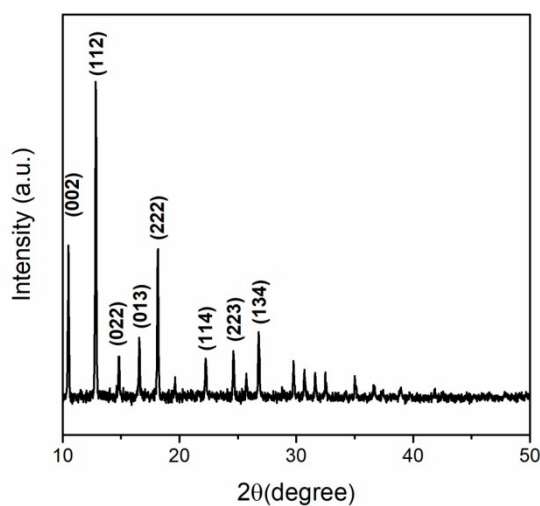


Fig. S1 XRD pattern of ZIF-67 nanocubes

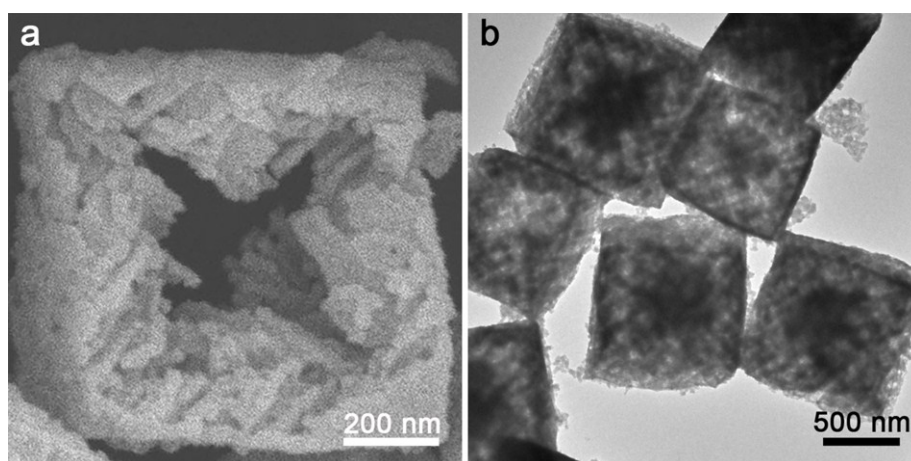


Fig. S2 (a) FESEM and (b) TEM images of the ZIF-67 nanoscaffolds.

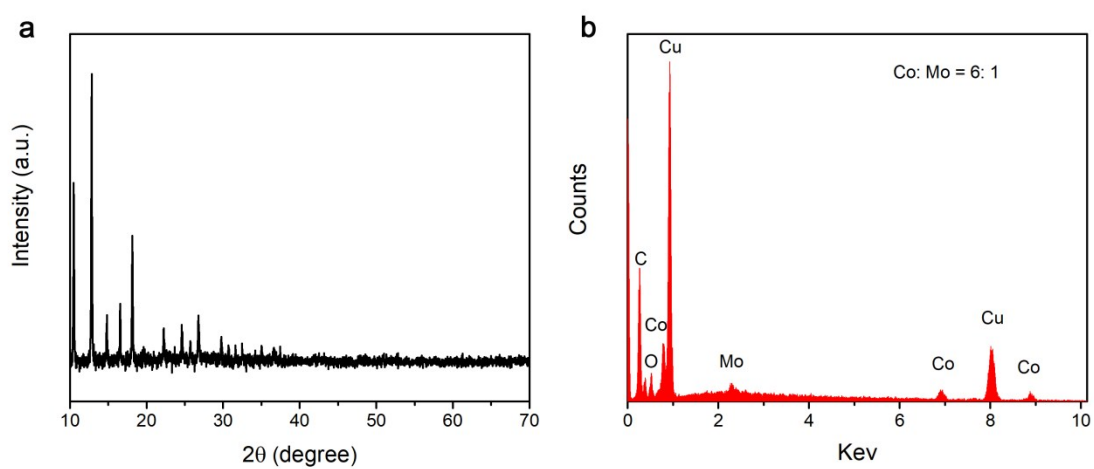


Fig. S3 (a) XRD pattern and (b) EDX spectrum of the ZIF-67 nanoscaffolds.

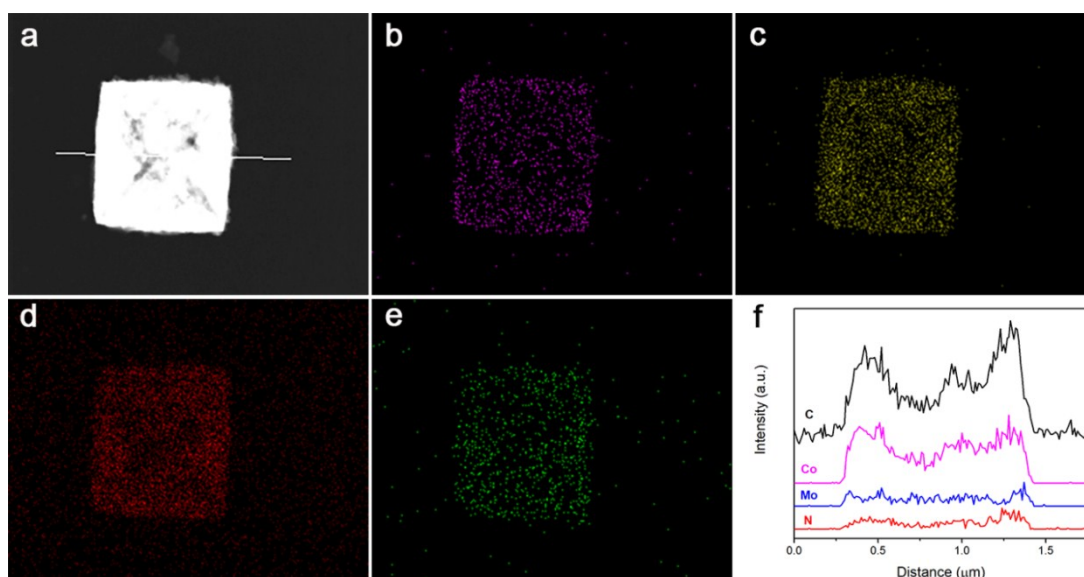


Fig. S4 (a) HAADF-STEM image of a ZIF-67 nanoscaffold, elemental mapping images of Co (b), Mo (c), C (d), and N (e) of the nanoscaffold show in (a), (f) elemental line scan of the nanoscaffold show in (a).

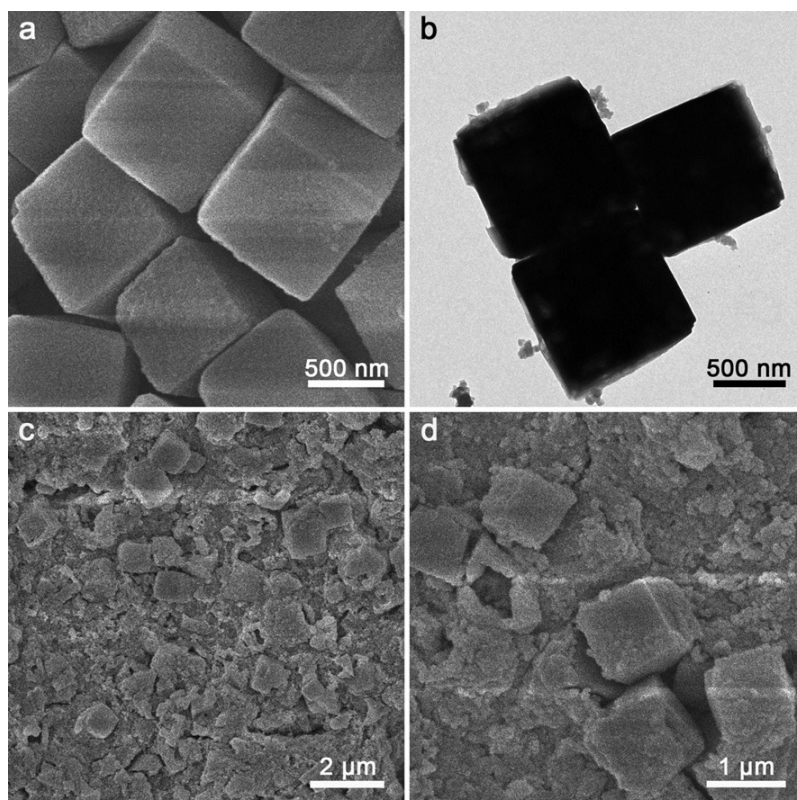


Fig. S5 (a) FESEM and (b) TEM images of the product (PDA@ZIF-67 nanocubes) without the addition of POM. (c,d) FESEM images of the product without the addition of dopamine.

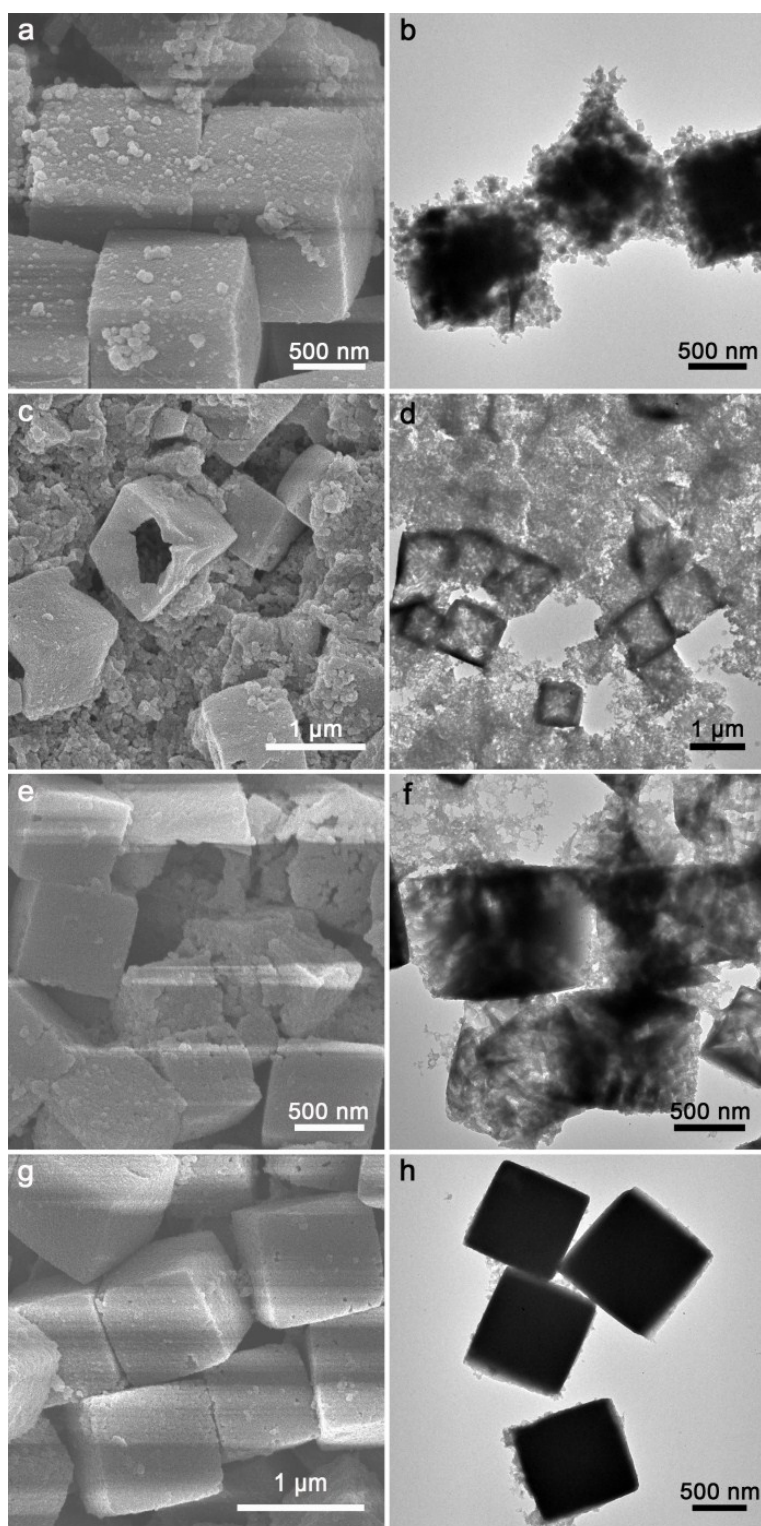


Fig. S6 (a, c, e, g) FESEM and (b, d, f, h) TEM images of the products with different contents of dopamine (DA) and POM. (a-b, 5 mg DA, 10 mg POM; c-d, 5 mg DA, 40 mg POM; e-f, 2.5 mg DA, 20 mg POM; g-h, 10 mg DA, 20 mg POM).

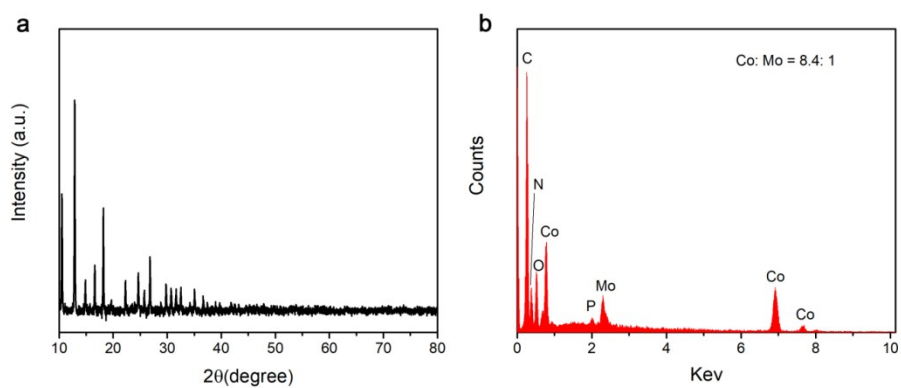


Fig. S7 (a) XRD pattern and (b) EDX spectrum of the ZIF-67 magic nanocubes.

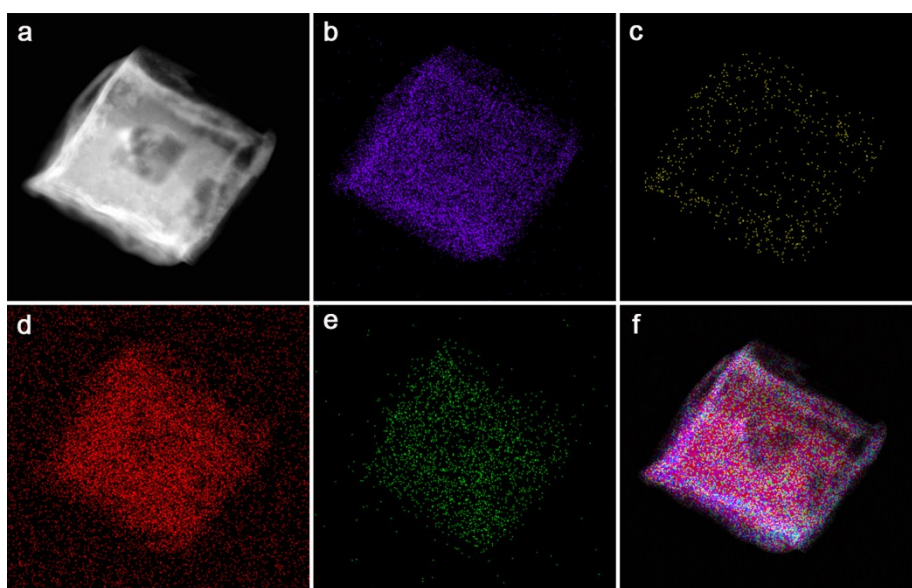


Fig. S8 (a) HAADF-STEM image of a ZIF-67 magic nanocube, elemental mapping images of Co (b), Mo (c), C (d), N (e), and overlap (f) of the magic cube show in (a).

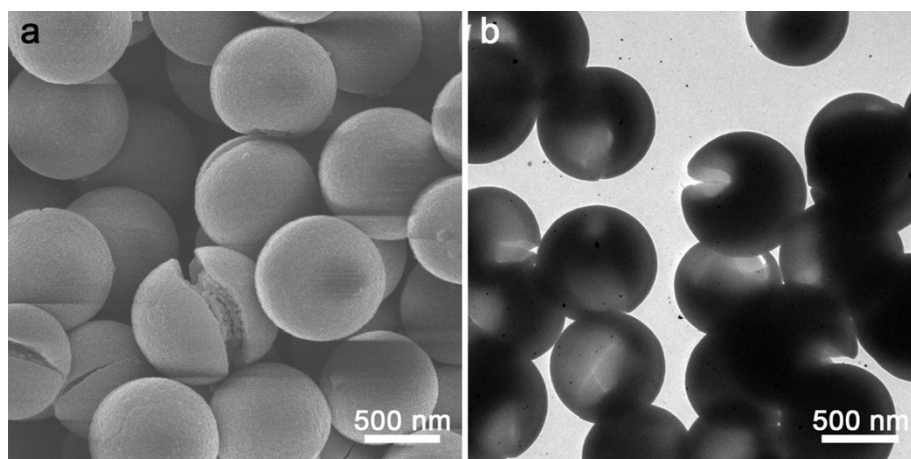


Fig. S9 (a) FESEM and (b) TEM images of the PDA-POM nanospheres.

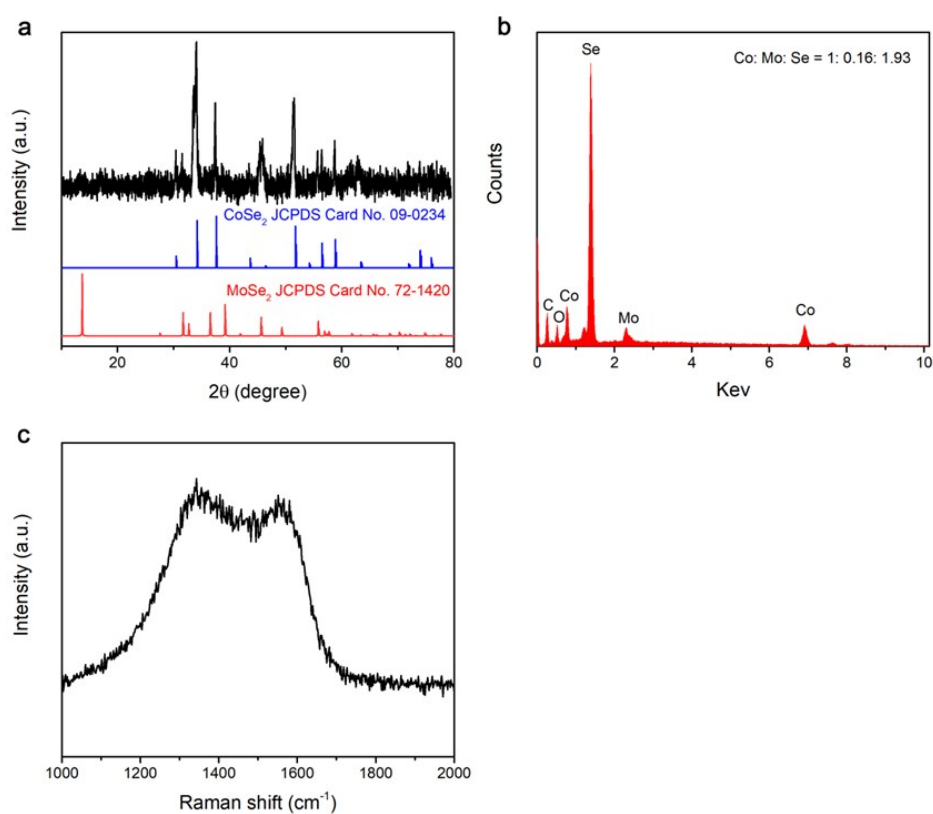


Fig. S10 (a) XRD pattern, (b) EDX spectrum, and (c) Raman spectrum of the CoMoSe@C nanoscaffolds.

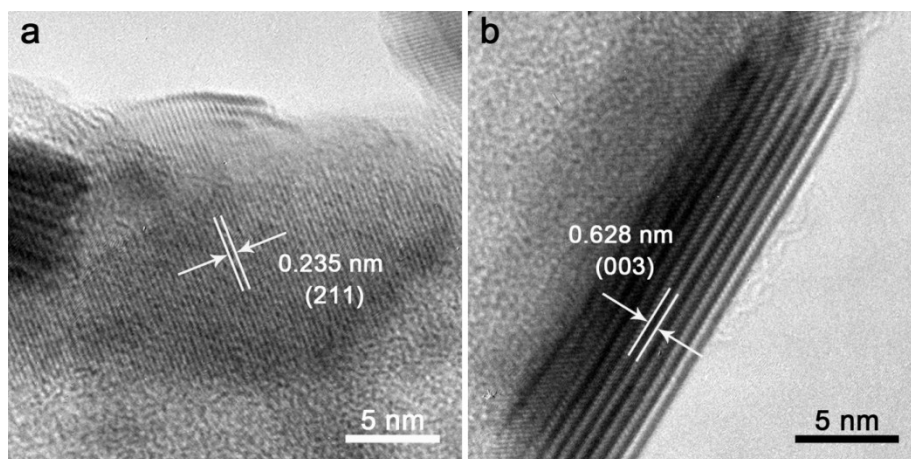


Fig. S11 (a,b) HRTEM images of the CoMoSe@C nanoscaffold.

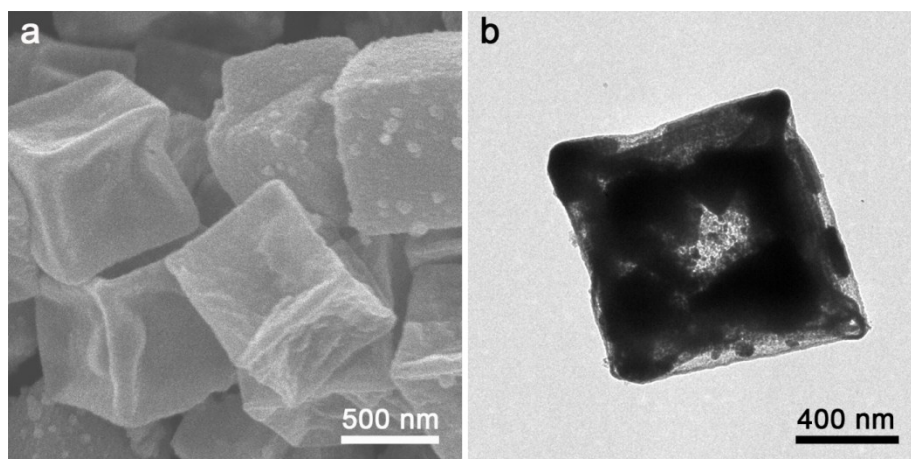


Fig. S12 (a) FESEM and (b) TEM images of the CoSe₂@C nanoboxes.

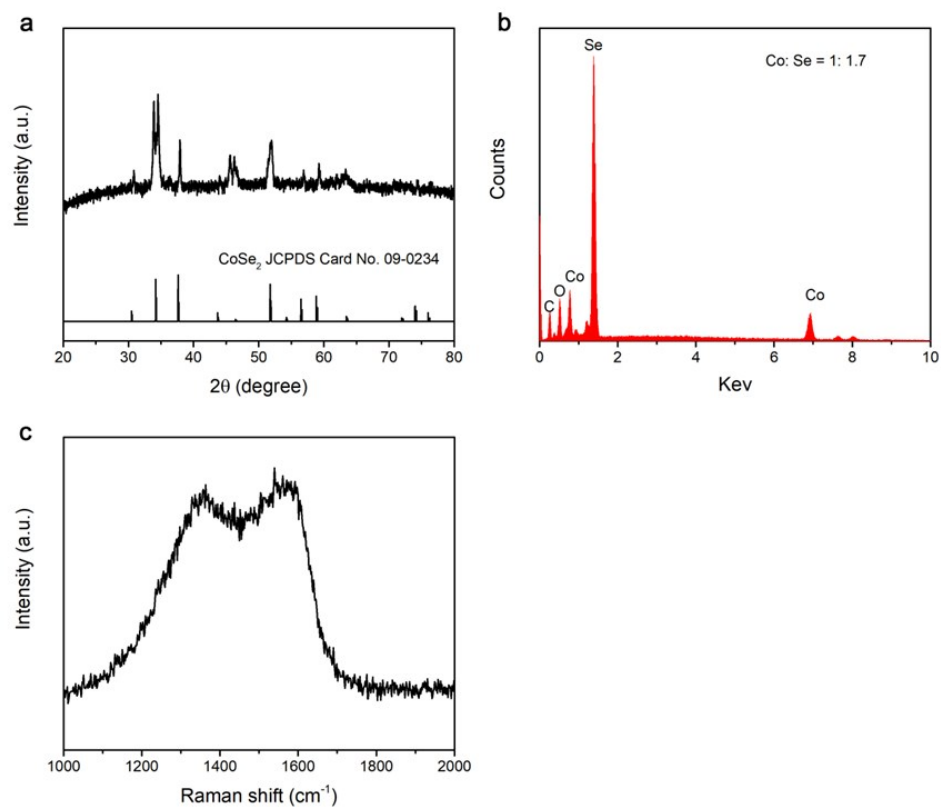


Fig. S13 (a) XRD pattern, (b) EDX spectrum, and (c) Raman spectrum of the $\text{CoSe}_2@\text{C}$ nanoboxes.

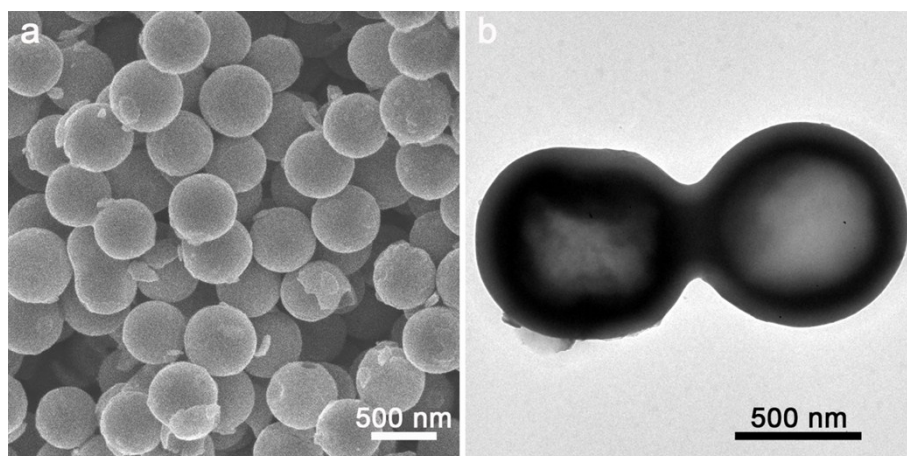


Fig. S14 (a) FESEM and (b) TEM images of the $\text{MoSe}_2@\text{C}$ hollow nanospheres.

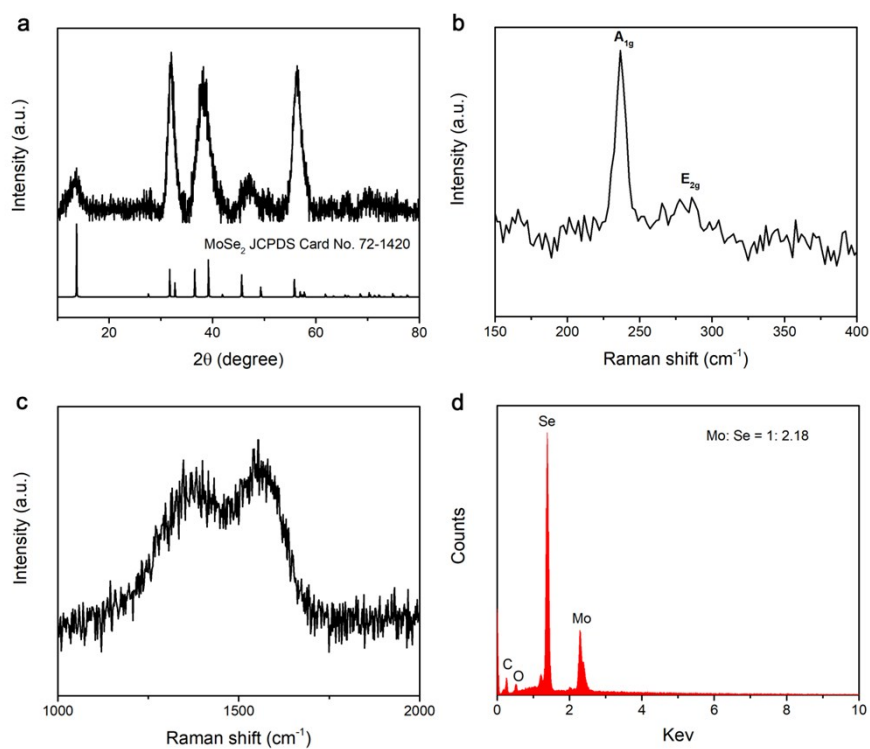


Fig. S15 (a) XRD pattern, (b,c) Raman spectrum, and (d) EDX spectrum of the MoSe₂@C hollow nanospheres.

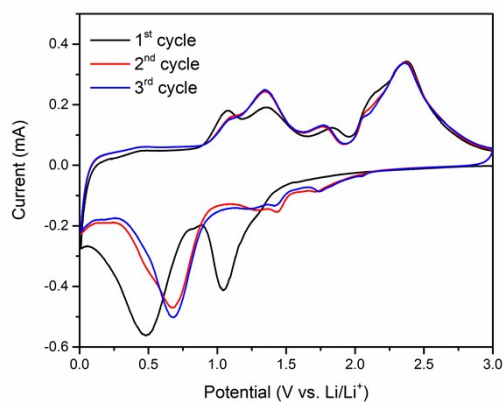


Fig. S16 CV curves of the CoMoSe@C nanoscaffolds in the voltage window of 0.0- 3.0 V vs. Li/Li⁺ at a scan rate of 0.2 mV s⁻¹.

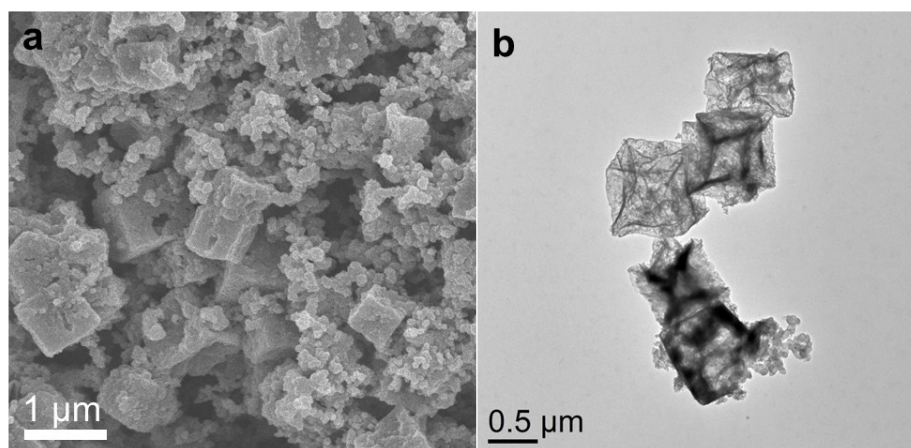


Fig. S17 (a) FESEM and (b) TEM images of the CoMoSe@C nanoscaffolds after cycling test.

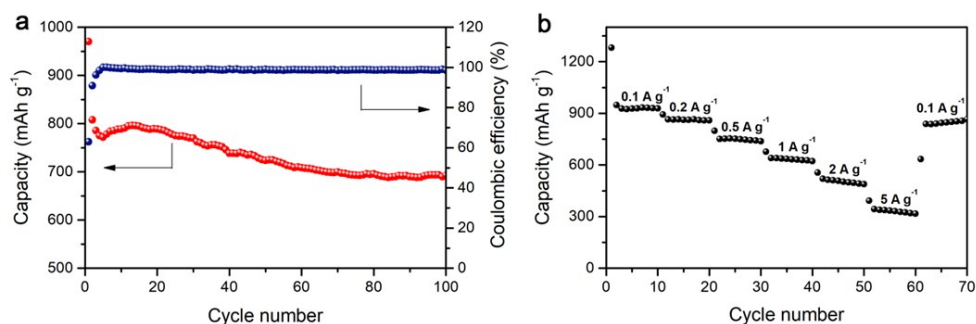


Fig. S18 (a) Cycling performance and (b) rate capability of the CoSe₂@C nanoboxes.

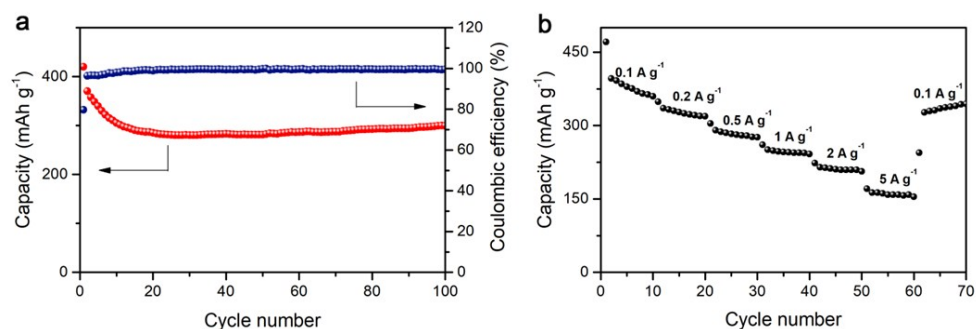


Fig. S19 (a) Cycling performance and (b) rate capability of the MoSe₂@C hollow nanospheres.

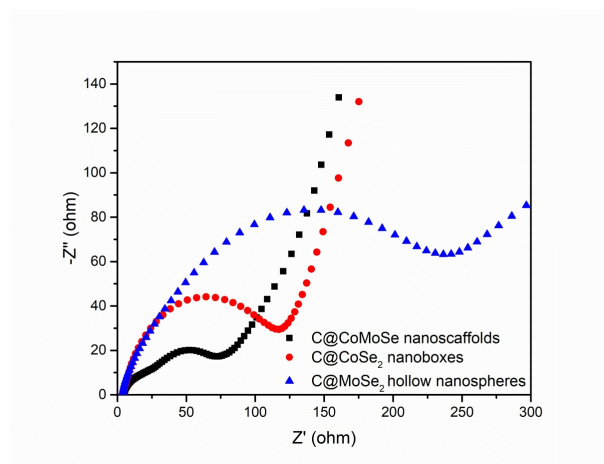


Fig. S20 Nyquist plots of the CoMoSe@C nanoscaffolds, CoSe₂@C nanocubes, and MoSe₂@C hollow spheres.